ASN NEURO RESEARCH ARTICLE

ASN NEURO 4(6):art:e00097.doi:10.1042/AN20120035

Neuroblast migration and $P2Y_1$ receptor mediated calcium signalling depend on 9-O-acetyl GD3 ganglioside

Marcelo F Santiago*,† and Eliana Scemes†1

*Instituto de Biofisica Carlos Chagas Filho, Universidade Federal do Rio de Janeiro, Rio de Janeiro, Brazil

†Dominick P. Purpura Department of Neuroscience, Albert Einstein College of Medicine, Bronx, NY 10461, U.S.A.

Cite this article as: Santiago MF and Scemes E (2012) Neuroblast migration and $P2Y_1$ receptor mediated calcium signalling depend on 9-O-acetyl GD3 ganglioside. ASN NEURO 4(6):art:e00097.doi:10.1042/AN20120035

ABSTRACT

Previous studies indicated that a ganglioside 9acGD3 (9-O-acetyl GD3) antibody [the J-Ab (Jones antibody)] reduces GCP (granule cell progenitor) migration *in vitro* and *in vivo*. We here investigated, using cerebellar explants of post-natal day (P) 6 mice, the mechanism by which 9acGD3 reduces GCP migration. We found that immunoblockade of the ganglioside with the J-Ab or the lack of GD3 synthase reduced GCP *in vitro* migration and the frequency of Ca^{2+} oscillations. Immunocytochemistry and pharmacological assays indicated that GCPs expressed $P2Y_1$Rs ($P2Y_1$ receptors) and that deletion or blockade of these receptors decreased the migration rate of GCPs and the frequency of Ca^{2+} oscillations. The reduction in $P2Y_1$-mediated calcium signals seen in Jones-treated and GD3 synthase-null GCPs were paralleled by $P2Y_1$R internalization. We conclude that 9acGD3 controls GCP migration by influencing $P2Y_1$R cellular distribution and function.

Key words: cerebellar granule cell, Jones antibody, GD3 synthase, $P2Y_1$ receptor, calcium signalling and neuronal migration.

INTRODUCTION

In the post-natal developing cerebellum, granule cell precursors [GCPs (granule cell progenitors)] migrate over radial glial fibres from the external granular layer through the molecular layer to reach their final position in the internal granular layer (Rakic, 1971); there, they differentiate into excitatory granule cells and integrate into the cerebellar circuitry (Hatten, 1999; Ito, 2006). Cerebellar granule cells are the most abundant type of neurons in the central nervous system (Herculano-Houzel, 2010) and defects in their genesis and/or migration cause severe dysfunction in motor balance and impairs the control of speech and movements of limb and eyes (Ben-Arie et al., 1997; Hong et al., 2000).

Many extracellular matrix components, glycoproteins and neurotrophic factors were described to influence neuroblast migration (O'Shea et al., 1990; Husmann et al., 1992; Zheng et al., 1996; Schwartz et al., 1997; Bates et al., 1999; Vaudry et al., 1999; Adams et al., 2002; Borghesani et al., 2002; Li et al., 2004; Cameron et al., 2007; Wilson et al., 2010). In addition, cell surface gangliosides have also been implicated in the migration of GCPs (Santiago et al., 2001, 2004).

Gangliosides are a subfamily of glycosphingolipids that contain at least one residue of sialic acid on the carbohydrate moiety (Yu et al., 2009, 2012). The expression levels of gangliosides in mouse brains change drastically during development (Ngamukote et al., 2007), with the peak expression of the ganglioside 9acGD3 (9-O-acetyl GD3) precisely correlating with times of most active neuronal motility and axonal outgrowth (Constantine-Paton et al., 1986; Mendez-Otero et al., 1988).

The amphipathic ganglioside molecules are preferentially localized in the outer leaflet of the cell membrane where they can be found within distinct microdomains that are important for several cell signalling pathways (Hakomori, 2002). However, knowledge about which signalling pathway(s) is affected by 9acGD3 remains speculative.

As the migration of neural progenitor cells has also been shown to be dependent on intracellular calcium transients (Komuro and Rakic, 1993, 1996, 1998; Yacubova and Komuro, 2002; Scemes et al., 2003; Kumada and Komuro, 2004; Agresti et al., 2005b; Agresti et al., 2005a; Striedinger et al., 2007), we evaluated whether the interference of 9acGD3-mediated neuronal migration affected Ca^{2+} signalling in GCPs derived from postnatal cerebellar explants.

[1]To whom correspondence should be addressed (email eliana.scemes@einstein.yu.edu).

Abbreviations: 9acGD3, 9-O-acetyl GD3; DAPI, 4′,6-diamidino-2-phenylindole; DMEM, Dulbecco's modified Eagle's medium; DPBS, Dulbecco's PBS; eGFP, enhanced green fluorescent protein; GCP, granule cell progenitor; GFAP, glial fibrillary acidic protein; J-Ab, Jones antibody; MAP, microtubule-associated protein; P2R, purinergic P2 receptor; WT, wild-type.

Here, we show for the first time that in mouse cerebellar neuroblasts, immunoblockade of 9acGD3 or the lack of this ganglioside reduce GCP migration rate and the frequency of $P2Y_1R$ ($P2Y_1$ receptor)-mediated spontaneous calcium oscillations. This reduction in calcium activity following 9acGD3 immunoblockade or its deletion is shown here to be paralleled by internalization of the $P2Y_1$ receptor. Our data reveal novel interactions between distinct signalling systems that influence the *in vitro* migration of neuroblasts.

MATERIAL AND METHODS

Animals

WT (wild-type) and the $P2Y_1$-null (B6.129P2-P2ry1^{tm1Bhk}/J) mice, originally generated by Dr Beverly Koller (University of North Carolina at Chapel Hill) were purchased from Jackson Laboratory and the GD3 synthase-null mice generated by Kawai et al. (2001) were a gift from Dr Steven Wakley (Department of Neuroscience, Albert Einstein College of Medicine). All animals were maintained in the animal facility at Albert Einstein College of Medicine. All animal handling and experimental protocols were approved by the Animal Care and Use Committee of the Albert Einstein College of Medicine.

Explants culture from early postnatal cerebellum

Methods for explant cultures of early postnatal murine cerebella have been previously described (Hockberger et al., 1987; Nagata and Nakatsuji, 1990; Santiago et al., 2001). Briefly, cerebella from post natal days 6 (P6) WT, $P2Y_1R$-null and GD3 synthase-null mice were quickly removed from skulls and placed in ice-cold DPBS (Dulbecco's PBS, pH 7.4; Cellgro). Cerebella were freed from meninges and choroid plexus, and the white matter and deep nuclei were gently removed. Small pieces of the remaining grey matter were dissected and chopped under a stereo microscope and rinsed in DMEM-F12 (Dulbecco's modified Eagle's medium nutrient mixture F12; Gibco, Invitrogen), supplemented with 5% of B27 (Gibco, Invitrogen) and 1% of antibiotics. Five to seven explants (398 ± 48 μm in diameter) were plated on glass bottom dishes (MatTek Co.) precoated with poly-D-lysine (10 μg/ml; Sigma) and laminin (40 μg/ml; Invitrogen). Explants plated with 50 μl of the culture medium on coated dishes were placed in an incubator (5% CO_2:95% air) at 37 °C for 30–40 min prior to addition of 1 ml of the culture medium and cultures were maintained till experimentation. Cerebellar explants were used within 2–4 days of culture.

Immunocytochemistry

Two-day adherent cerebellar explants were fixed for 15 min with 4% paraformaldehyde (EMS) diluted in DPBS, washed three times in DPBS and then incubated for 30 min with Triton X-100 (Sigma) (0.01% for immunostaining with anti-gangliosides antibodies; 0.4% all other antibodies) and 10% normal goat serum (Sigma) diluted in DPBS. Samples were incubated overnight with either monoclonal mouse IgG anti-MAP-2 (microtubule-associated protein 2) (1:200; Sigma), polyclonal rabbit anti-GFAP (glial fibrillary acidic protein; 1:500; Sigma), polyclonal rabbit anti-$P2Y_1R$ (1:200; Alomone Labs) or monoclonal mouse IgM anti-A2B5 (1:1000; R&D Systems) that recognizes the c-series gangliosides (Eisenbarth et al., 1979). The monoclonal mouse IgM Jones (binds to 9acGD3; 1:10) developed by Dr M. Constantine-Paton (Constantine-Paton et al., 1986) was obtained from Developmental Studies Hybridoma Bank developed under the auspices of the NICHD and maintained by The University of Iowa, Department of Biological Sciences, Iowa City, IA. After several washes with DPBS, explants were incubated with Alexa Fluor® 488 or 594-conjugated goat anti-mouse IgG or IgM or anti-rabbit antibodies (1:1000; Molecular Probes, Invitrogen). After 2 h incubation with secondary antibodies, at room temperature, the dishes were washed three times in DPBS and mounted with VectaShield with DAPI (4′,6-diamidino-2-phenylindole; Vector Labs.). Immunostaining was visualized and imaged using proper filter sets using an inverted epifluorescence microscope (Eclipse TE2000-S; Nikon) connected to a CCD camera (Orca-ER; Hamamatsu) using Metafluor software (Universal Imaging Systems) or under a confocal microscope system configured with a *xy*-motorized inverted stage, 12 laser lines and 32-channel spectral imaging (Zeiss Duo V2).

Intracellular calcium transients

Two-day-old cerebellar explants were loaded for 30 min at 37 °C with 1–2 μM Flou-3-AM (Molecular Probes, Invitrogen) and then bathed in DPBS. Loaded cells were imaged on an epifluorescence microscope (Eclipse TE2000-S; Nikon) connected to a CCD camera (Orca-ER; Hamamatsu). Fluo-3 was excited/detected (488 nm/510–550 nm) at 2 Hz using FITC filters and shutter (Lambda DG-4 Diaphot, Sutter Instruments Co.) driven by a computer through Metafluor software. Morphological aspects of neuroblasts were used to define regions of interest from which relative Fluo-3 fluorescence intensity (F/F_0) was measured. Spontaneous calcium oscillations, cut-off at 2% F/F_0, were recorded over a period of 10 min. For pharmacological assays, F/F_0 (cut-off at 5%) was measured before and during bath application of P2R (purinergic P2 receptor) agonists, as described previously (Scemes et al., 2003). The following P2R agonists and antagonist were used: ATP (1 μm; Sigma), UTP (1 μM; Sigma), 2-methylthio-ATP (1 μM; 2MeSATP; Calbiochem), α,β-methylene-ATP (1 μM; αβMeATP; Sigma) and 3′-O-4-benzoylbenzoyl-ATP (300 μM; BzATP; Sigma), KN62 (1 μM; Sigma) and MRS 2179 (10 or 100 μM; Tocris Cookson). Similar experiments were performed on WT cerebellar explants treated for 2 h with Jones (1 ng/μl) and A2B5 (1 ng/μl) monoclonal antibodies and from those derived from $P2Y_1$-null and GD3 synthase-null mice.

Quantification of neuronal migration

To evaluate the distance migrated by GCPs, P6 mouse cerebellar explants were plated on poly-D-lysine/laminin-coated glass-bottomed dishes containing DMEM-F12 with or without 1 ng/ml J-Ab (Jones antibody), 1 ng/ml A2B5 antibody, 20 mU/ml *Clostridium perfringens* neuraminidase (N'ase; Sigma), 1 ng/ml R24 antibody, or 100 μM MRS 2179, which were added to the cultures at the moment and 24 h after plating. The migration distance attained 48 h after plating was obtained by measuring the distance of the foremost cell bodies (mean of three measurements per explant) to the border of explants in the conditions described above. For that, live explants were imaged under DIC optics (Eclipse TE2000-S; Nikon) and distances were measured using ImageJ software.

Transfection with $P2Y_1$ receptor cDNA and fluorescence intensity profile analysis

Two-day-old cerebellum explants from P6 mice plated on poly-D-lysine/laminin-coated glass-bottomed dishes were transfected with 6 μg/ml eGFP (enhanced green fluorescence protein)-$P2Y_1$R cDNA using Optifect (Invitrogen) as previously described (Scemes et al., 2003). At 36–40 h after transfection, eGFP-$P2Y_1$R expression on live migrated GCPs was visualized using a confocal microscope (Zeiss Duo V2) and eGFP-positive GCPs were imaged through the *z*-plane using a 40×/1.2 N.A. water immersion objective. Images were taken before and 2 h after exposure of the explants to 1 ng/ml Jones, 1 ng/ml A2B5 or control medium. During this incubation period, cultures were maintained in an incubator (5% CO_2:95% air) at 37°C. Fluorescence intensity profile analysis of eGFP-$P2Y_1$R distribution was performed using ImageJ software. When indicated, fluorescence intensity profile analysis of native $P2Y_1$Rs was obtained from untransfected neuroblasts immunostained with anti-$P2Y_1$R antibody.

RESULTS

In vitro characterization of progenitors derived from P6 mouse cerebellar explants and expression of 9acGD3 ganglioside

Two days after plating P6 WT mouse cerebellar explants on laminin-coated coverglasses, an extensive number of radially migrated cells were observed around the explants (Figure 1A). At least two distinct types of migrated cells were easily recognized by their morphological aspects under DIC optics: a predominant population of cells with small (~8 μm) elongated cell bodies (arrows in Figures 1A and 1A′) and a smaller population of cells with larger (~15 μm) flat polygonal-shaped cell bodies (arrowheads in Figures 1A and 1A′). The majority of the migrated cells (small elongated) and outgrowing processes were from the neuronal lineage as revealed by a strong MAP-2 staining (Figures 1B and 1D) and class III β-tubulin (data not shown), while the other population of cells were GFAP-positive (larger cell bodies and nuclei; arrowhead in Figure 1D) with radially oriented processes in close proximity with the explant borders (<150 μm). This result is in agreement with a previous report indicating that approximately 95% of cells migrated from cerebellar explants are GCPs (Hockberger et al., 1987). Immunostaining with J-Ab revealed a strong and punctate expression of the ganglioside 9acGD3 in virtually all GCPs (Figure 1C).

Immunoblockade of 9acGD3 reduces the rate of migration and inhibits spontaneous calcium oscillations of GCPs

It has been previously shown that binding of J-Ab to the ganglioside 9acGD3 impairs the migration of rat cerebellar GCPs *in vitro* and *in vivo* (Santiago et al., 2001, 2004). To evaluate the extent to which this effect was also reproduced in mice, we incubated mouse cerebellar explants with J-Ab (1 ng/ml) for 48 h and then measured the distance of GCP migration. After 2 days in culture, control explants displayed a wave front of migrating cells extending as far as 506±19 μm from the border of the explants (Figure 1F; $n=6$ independent experiments). Long-term J-Ab incubation significantly decreased the distance migrated by GCPs from the explants (253±11 μm; $n=4$ independent experiments) compared with that measured from control, untreated explants ($P<0.001$). To control for possible non-specific effects of the IgM portion of J-Ab, we used the A2B5 antibody (isotype IgM) which recognizes c-series gangliosides (Eisenbarth et al., 1979; Ngamukote et al., 2007) that are expressed in these neuroblasts. As a positive control indicative of the contribution of 9acGD3 to GCP migration, we used neuraminidase, an enzyme that cleaves terminal sialic acids from glycoconjugates (Ledeen and Yu, 1982; Taube et al., 2009). As shown in Figure 1(F), no significant difference in migration distance was detected between A2B5-treated (1 ng/ml) explants (580±37 μm; $n=4$ independent experiments) and control, untreated explants, while explants treated with neuraminidase (N'ase; 20 mU/ml for 48 h) showed a significant reduction of more than 50% (249±38 μm; $n=3$ independent experiments) of the migration distance of GCPs from the explants (Figure 1F; $P<0.001$). As previously reported for P19 neural stem cells (Santiago et al., 2005), the anti-GD3 antibody, R24 antibody (1 ng/ml) did not affect the migration of cerebellar neuroblasts (control: 491.4±36.24 μm, $n=10$ explants; R24: 510.7±21.66 μm, $n=26$ explants; $P=0.65$, unpaired *t* test).

Thus, these results indicate that 9acGD3 plays an important role during mouse cerebellar neuroblast migration, as previously reported for rat GCP migration (Santiago et al., 2001, 2004).

In order to gain insight into the mechanisms by which J-Ab affects neuroblast migration, we first investigated whether immunoblockade of 9acGD3 affected spontaneous calcium transients in GCPs, given that the rate of migration of progenitor cells has been proposed to be directly correlated

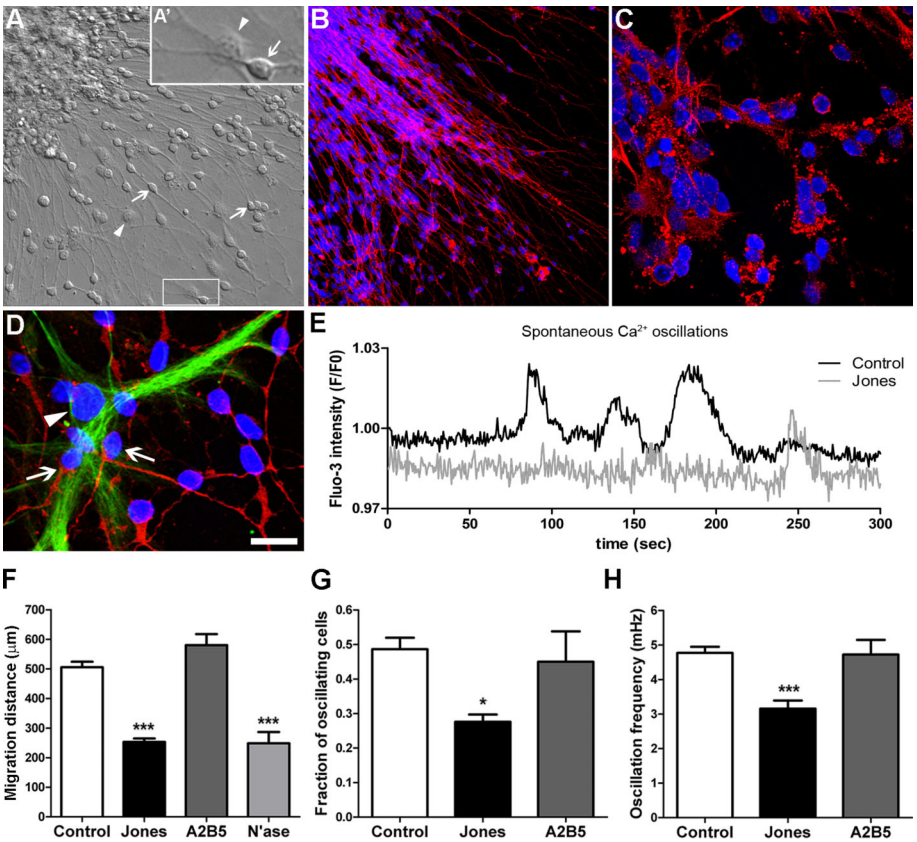

Figure 1 **Impact of 9acGD3 immunoblockade on GCPs migration and spontaneous calcium oscillations**

(**A**) DIC (differential–interferential contrast) images obtained from a cerebellar explant (upper-left corner) showing migrated cells after 2 days *in vitro*. GCPs (arrows) and glial cells (arrowheads) found in the migratory halo around the explant can be easily distinguished from one another by their morphology under DIC optics (**A′** inset). The majority of cells and processes are from the neuronal lineage as indicated by the expression of MAP-2 (**B**). Virtually all emigrated GCPs express the ganglioside 9acGD3 as indicated by the punctuated membrane staining with J-Ab (**C**). Confocal image in (**D**) illustrates glial GFAP-positive (green) radial processes and MAP-2-positive (red) GCPs in close proximity to each other (arrows in **D**). Nuclei in (**B–D**) were counterstained with DAPI. Scale bar: **A**=30 μm; **B**=50 μm; **C**=20 μm; **D**=15 μm. Traces in (**E**) are examples of spontaneous calcium oscillations continuously recorded for 5 min from two GCPs loaded with the calcium indicator Fluo-3-AM that were untreated (black trace) and treated (light-grey trace) with J-Ab (1 ng/μl for 2 h). (**F–H**) Bar histograms showing the means±S.E.M. values of the migration distance (**F**), of the fraction of cells displaying spontaneous calcium oscillation (**G**), and the frequency of spontaneous calcium transients (**H**) of GCPs untreated (white bars) and treated with Jones (black bars) and with A2B5 (grey bars) antibodies. N′ase corresponds to neuraminidase-treated (20 mU/ml; light-grey bar) group. ***$P<0.001$; *$P<0.05$; ANOVA, followed by Tukey's multiple comparison test.

with the frequency of spontaneous intracellular calcium oscillations (Komuro and Rakic, 1996; Scemes et al., 2003). To that end, we monitored spontaneous intracellular calcium oscillations in Fluo-3 AM (acetoxymethyl ester) loaded cells migrated from 2-day-old explants treated for 2 h with J-Ab (1 ng/ml). Under control conditions, 49% (0.49±0.03: 202 of 412 cells; $n=5$ independent experiments; Figure 1G) of migrated GCPs displayed spontaneous calcium transients (black trace in Figure 1E). The mean frequency of spontaneous calcium oscillations was 4.77±0.18 mHz, ranging from 1 to 10 mHz (Figure 1H). J-Ab treatment (light-grey trace in Figure 1E) significantly decreased both the fraction of cells displaying spontaneous Ca^{2+} oscillations (0.28±0.02: 111 of 396 cells; $n=4$ independent experiments; $P<0.05$; Figure 1G) and the frequency of Ca^{2+} transients (3.16±0.23 mHz; $P<0.01$; Figure 1H). To evaluate whether the effects of J-Ab on calcium transients were due to a non-specific effect of the IgM portion of the antibody, we performed similar experiments as described above, but using the A2B5 antibody. Compared with control condition, treatment with A2B5 antibody (1 ng/ml for 2 h) did not significantly ($P>0.05$) alter either the fraction of cells with Ca^{2+} oscillations (0.45±0.09: 167 of 371 cells; $n=4$ independent experiments; Figure 1G) or the frequency of these calcium transients (4.73±0.42 mHz; Figure 1H).

Impaired neuroblast migration and spontaneous calcium oscillations in GD3S-null mice

To evaluate further the contribution of the ganglioside 9-OacGD3 to GCP migration, we used GD3S-null mice, which lack all the GD3 series of gangliosides, including the 9-OacGD3, as shown by the lack of Jones immunostaining on P6 derived cerebellar explants (Figures 2A–2C).

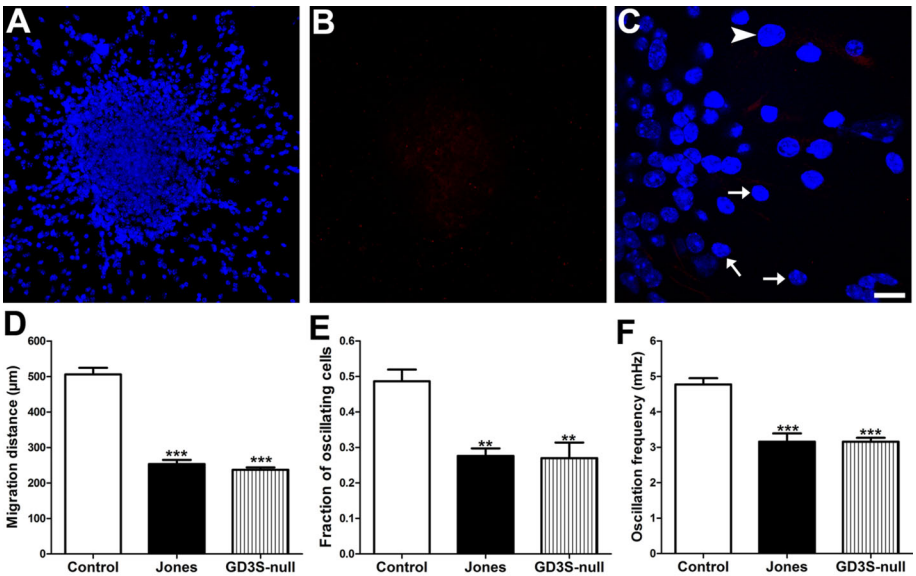

Figure 2 **Reduced migration and calcium oscillations in the GD3 synthase null mice**
(**A–C**) Fluorescence images obtained from cerebellar explants of GD3 synthase null mice, showing lack of 9acGD3 immunstaning (**B**, **C**) in both glia (arrowhead in **C**) and neuroblasts (arrows in **C**); nuclei were counterstained with DAPI (**A**, **B**). (**D–F**) Bar histograms showing the means ± S.E.M. values of the fraction of the migration distance (**D**) of WT GCPs untreated (white bars) and treated with J-Ab (black bars) and in untreated GD3-null neuroblasts (grey bars), and of cells displaying spontaneous calcium oscillation (**E**), the frequency of spontaneous calcium transients (**F**). ***$P<0.001$; **$P<0.01$; ANOVA, followed by Tukey's multiple comparison test.

We found a significant reduction of the migration distance of GD3S-null neuroblasts compared with that recorded from WT cells (502.7 ± 44.0 μm, $n=9$ explants, GD3S KO (knockout): 237.1 ± 6.7 μm, $n=54$ explants; Figure 2D). Moreover, the distances migrated by GCPs derived from GD3S-null mice were similar to those measured from Jones treated WT cells (J-Ab: 253.1 ± 22.7 μm, $n=15$ explants; Figure 2D); J-Ab treatment did not affect the migration of GD3S-null neuroblasts (GD3S KO 237.1 ± 6.7 μm; J-Ab GD3S KO: 253.0 ± 18.7 μm, n = 14 explants; $P>0.05$, *t* test).

Similar to what was recorded from Jones-treated WT GCPs, both the fraction of active cells (0.27 ± 0.045, $n=6$ independent experiments; Figure 2E) and the frequency of spontaneous calcium oscillations (3.16 ± 0.01 mHz, $n=6$ experiments; Figure 2F) of GD3S-null GCPs were also significantly ($P<0.0001$, *t* test) decreased compared with WT cells.

Thus, these results strongly suggest that one possible mechanism by which the immunoblockade of the ganglioside 9-OacGD3 affects neuroblast migration is through a pathway involving spontaneous calcium oscillations.

GCPs express functional $P2Y_1$Rs

P2R-mediated calcium oscillations have been reported to contribute to spontaneous calcium oscillations and to neural progenitor cell migration (Scemes et al., 2003; Agresti et al., 2005b; Liu et al., 2008). Mature granule cells express several types of P2Rs (Hervas et al., 2003; Amadio et al., 2007); however, very little is known about the functional expression of these receptors in early stages of cerebellar development, especially in GCPs. To that end, we measured intracellular calcium transients induced by P2R agonists in Fluo-3-AM loaded GCPs emigrated from 2-day-old explants. Bath application of the broad spectrum P2R agonist ATP (1 μM) induced an 11% ± 0.1-fold increase in intracellular calcium in 32% (108 of 338 cells; $n=4$ independent experiments) of recorded cells (Figure 3A). The $P2Y_1$R-specific agonist, 2MeSADP (1 μM), induced a similar elevation in intracellular calcium transients (1.16 ± 0.01-fold change in Fluo-3 fluorescence intensity) in 45% of the cells (135 of 299 cells; $n=4$ independent experiments; black trace in Figure 3B). To further test for the involvement of the $P2Y_1$R, we used MRS 2179 (10 μM for 5 min), a specific $P2Y_1$R antagonist. Under this condition, cytosolic calcium elevations induced by 1 μM 2MeSADP (light-grey trace in Figure 3B; $n=3$ independent experiments) were completely abolished. By contrast, bath application of 1 μM UTP (a $P2Y_{2/4}$ receptor agonist; $n=2$ independent experiments), 1 μM $\alpha\beta$MeATP (a broad spectrum P2XR agonist; $n=4$ independent experiments), or 300 μM BzATP (a $P2X_7$ receptor agonist; $n=2$ independent experiments) did not significantly increase intracellular calcium levels of GCPs (Figures 3C–3E, respectively).

These pharmacological assays indicate that $P2Y_1$R is likely the main purinergic receptor subtype expressed in GCPs. To test for the presence of these receptors in 2-day-old GCPs, P6 cerebellar explants were immunostained with an anti-$P2Y_1$R antibody and the expression and cellular distribution of these receptors analysed by confocal microscopy. Figure 3(F) shows that GCPs express the $P2Y_1$ purinergic receptor. An orthogonal view obtained from a *z*-section confocal

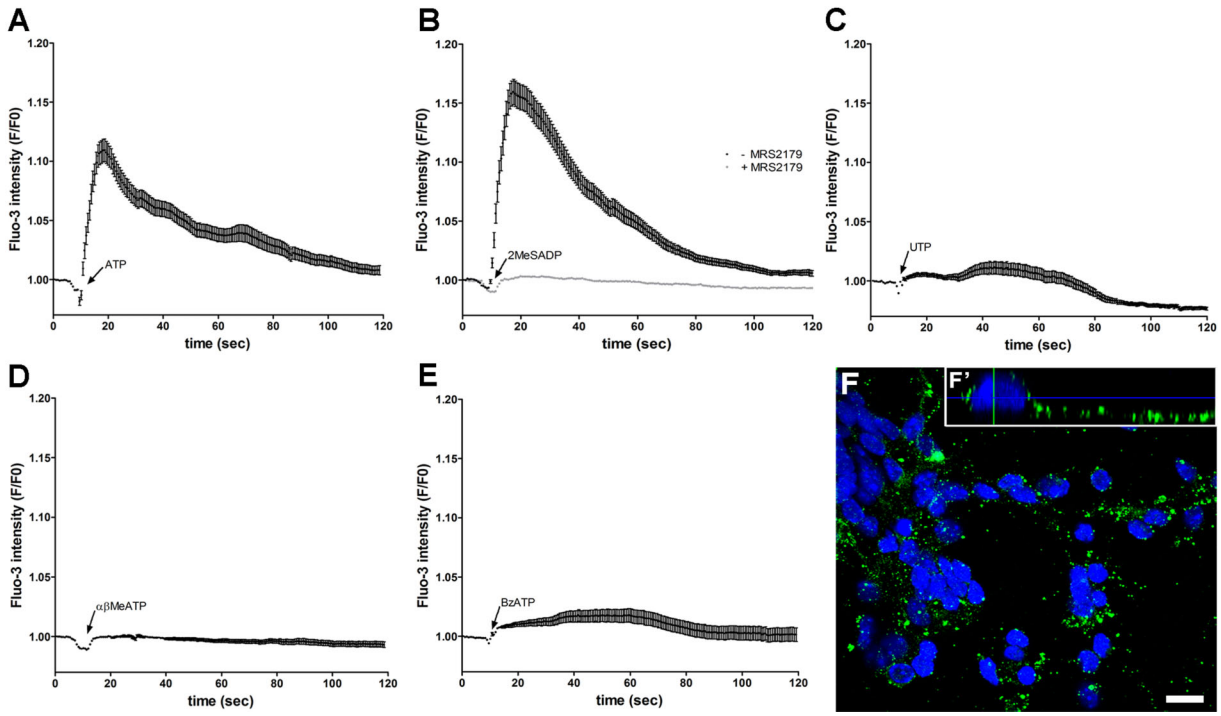

Figure 3 **GCPs migrated from P6 cerebella express functional $P2Y_1Rs$**
(**A**–**E**) Graphs showing the time course of intracellular calcium changes induced by bath application of (**A**) 1 μM ATP, (**B**) 1 μM 2MeSADP in the absence (black trace) and presence of MRS 2179 (10 μM; light-grey trace), (**C**) 1 μM UTP, (**D**) 1 μM $\alpha\beta$MeATP and (**E**) 300 μM BzATP. (**F**) Confocal image showing the cellular distribution of $P2Y_1R$ in GCPs. (**F′**) Shows a high magnification of an orthogonal view obtained from *z*-reconstruction of confocal images displaying punctated expression of the $P2Y_1R$ surrounding the cell body and along the neurite of a GCP. Nuclei were counterstained with DAPI (blue in **F** and **F′**). Scale bar: **F**=10 μm and **F′**=4 μm.

reconstruction revealed the expression of $P2Y_1R$ along the neurites of migrated GCPs (Figure 3F′).

Contribution of $P2Y_1R$ to spontaneous calcium oscillations and migration of GCPs

Evidence that $P2Y_1R$ contributes to GCPs spontaneous calcium oscillations was obtained by pharmacological means and the use of $P2Y_1$-null mice. Compared with control conditions, the $P2Y_1R$ antagonist MRS 2179 (100 μM for 2 h) significantly decreased both the fraction of cells with spontaneous calcium oscillations (from 0.49±0.03 [202 of 412 cells] to 0.27±0.07 [68 of 260 cells]; n=3 independent experiments; P<0.01; Figure 4A) and the frequency of these oscillations (from 4.77±0.18 mHz to 2.44±0.16 mHz; n=3 independent experiments; P<0.01; Figure 4B). In $P2Y_1R$-null cerebellar explants, a significantly lower fraction of emigrated GCPs (0.19±0.01 [144 of 762 cells]; n=4 independent experiments; P<0.001; Figure 4A) displayed spontaneous calcium transients when compared with the WT cells. Moreover, the frequency of these events was also significantly lower in $P2Y_1R$-null GCPs (2.30±0.07 mHz; n=4 independent experiments; P<0.01; Figure 4B) compared with that of WT cells. Furthermore, both the fraction of cells displaying spontaneous calcium oscillations and the frequency of these calcium activities recorded from the $P2Y_1R$-null explants were similar to those measured from WT cells treated with the $P2Y_1$ antagonist MRS 2179 (P>0.05; Figures 4A and 4B). Differently from what we recorded from WT GCPs, J-Ab treatment of $P2Y_1R$-null neuroblasts did not further decrease the fraction of cells displaying spontaneous calcium oscillations (0.17±0.01 [75 of 437 cells]; n=4 independent experiments) or the frequency of these calcium activities (2.33±0.17 mHz; n=4 independent experiments) recorded from the $P2Y_1R$-null explants.

To further examine the contribution of extracellular purine nucleotides to spontaneous calcium transients, we measured calcium transients in WT cells treated with the ATP degrading enzyme apyrase (5 U/ml for 5 min). Under this condition, both the fraction of cells displaying spontaneous calcium oscillations (0.11±0.03 [45 of 400 cells]; n=4 independent experiments; Figure 4A) and the frequency of these oscillations (2.62±0.49 mHz; n=4 independent experiments; Figure 4B) were greatly attenuated when compared with control, untreated cells (P<0.01).

The extent to which $P2Y_1R$-mediated spontaneous calcium oscillations correlates with the migration distance of WT GCPs was evaluated pharmacologically using the $P2Y_1R$-specific antagonist MRS 2179 and by using $P2Y_1$-null GCPs. Prolonged (48 h) blockade of $P2Y_1R$ with MRS 2179 (100 μM)

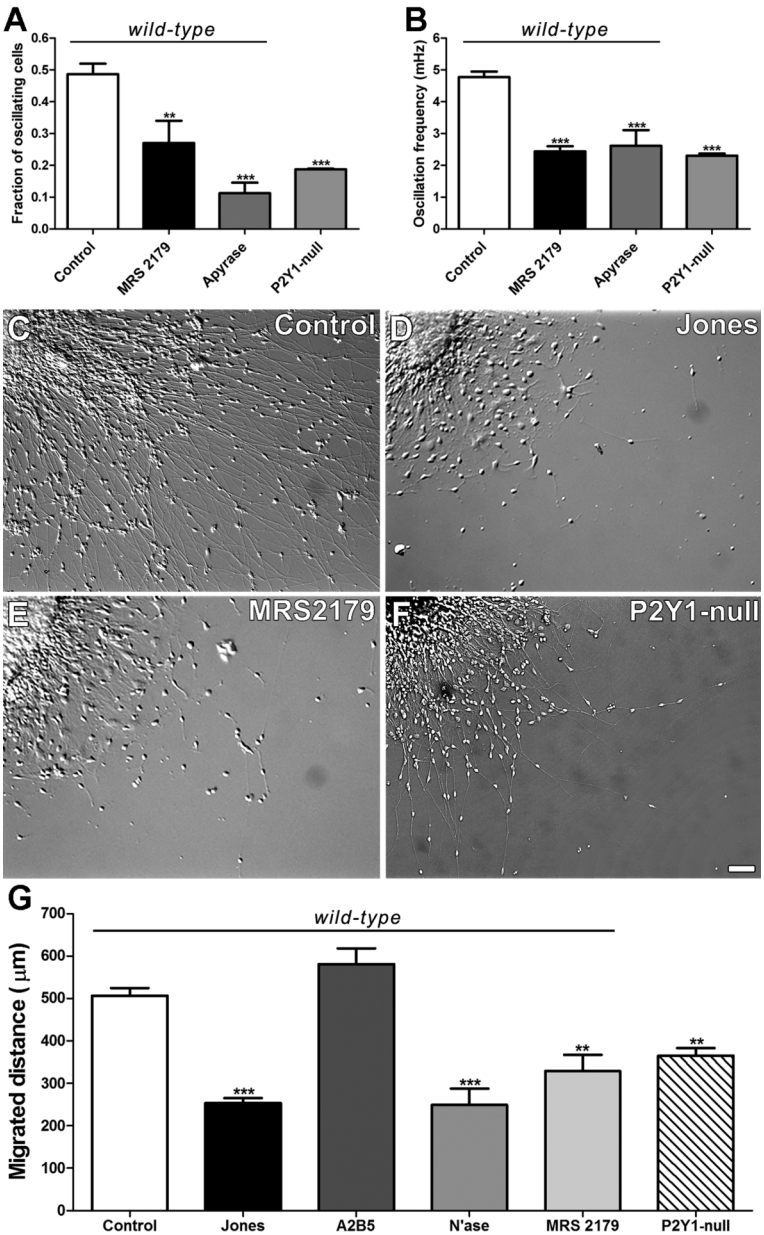

Figure 4 **P2Y$_1$R regulates GCPs spontaneous calcium oscillations and migration**
(**A**, **B**) Bar histograms showing the means ± S.E.M. values of (**A**) the fraction of cells and (**B**) the frequency of spontaneous calcium oscillations recorded from WT and P2Y$_1$R-null GCPs in the absence and presence of MRS 2179 (100 μM for 2 h) and apyrase (5 U/ml for 5 min). (**C–F**) DIC images from cells emigrated from 2-day-old WT untreated (**C**), treated for 48 h with (**D**) J-Ab or with (**E**) MRS 2179 and P2Y$_1$R-null untreated (**F**) explants. (**G**) Bar histograms showing the means ± S.E.M. values (at least three independent experiments) of the migration distance of GCPs from WT and P2Y$_1$R-null untreated and WT exposed for 48 h to Jones (1 ng/ml), to neuraminindase (N'ase: 20 mU/ml) and to MRS 2179 (100 μm). ***$P<0.001$; **$P<0.01$ (ANOVA, followed by Tukey's multiple comparison test). Scale bar: 30 μm.

significantly reduced the migration distance of GPCs (329 ± 38 μm; $n=3$ independent experiments; $P<0.01$; Figures 4C–4G) compared with control (506 ± 19 μm; $n=6$ independent experiments; Figures 4C, 4E and 4G) and to A2B5-treated (580 ± 37 μm; $n=4$ independent experiments; Figure 4G) explants. Similarly to MRS 2179-treated cells, the distance migrated by P2Y$_1$R-null GCPs was also reduced (364 ± 19 μm; $n=4$ independent experiments; $P<0.01$; Figures 4F and 4G). The short migration distances of GCPs treated with MRS 2179 and that of P2Y$_1$-null cells were similar ($P>0.05$) to those measured from J-Ab- (253 ± 11 μm; $n=4$ independent experiments; Figures 4D and 4G) and neuraminidase-treated explants (249 ± 38; $n=3$ independent experiments; Figure 4G). Moreover, J-Ab treatment

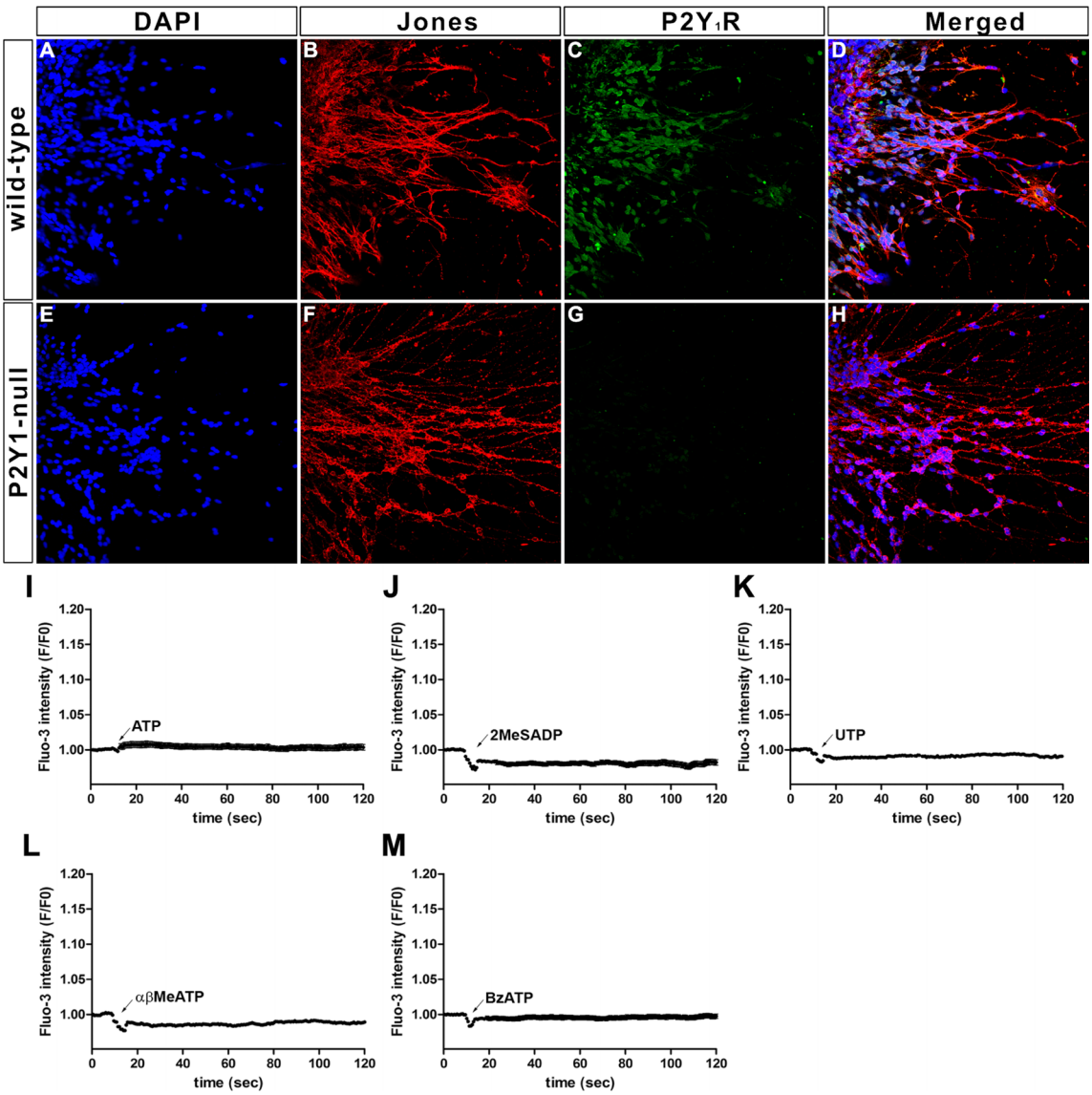

Figure 5 **Lack of $P2Y_1R$ immunoreactivity and agonist-induced calcium mobilization in $P2Y_1R$- null cerebellar explants**
WT (**A–D**) and $P2Y_1R$-null (**E–H**) P6 cerebellar explants were fixed after 2DIV, immunostained with Jones (red) and anti-$P2Y_1$ (green) antibodies and imaged by confocal microscopy at low magnification. Nuclei were stained with DAPI (blue). Note that in the WT progenitors the majority of emigrated cells express 9acGD3 (**B**) and $P2Y_1Rs$ (**C**). In $P2Y_1R$-null cells, the expression of the ganglioside is not altered (**F**) but the expression of $P2Y_1Rs$ is completely abolished (**G**). (**D**, **H**) Show DAPI, Jones and $P2Y_1R$ merged images. Scale bar: **A–H**=80 μm. (**I–M**) Graphs showing the time course of intracellular calcium changes induced by bath application of (**I**) 1 μM ATP, (**J**) 1 μM 2MeSADP, (**K**) 1 μM UTP, (**L**) 1 μM $\alpha\beta$MeATP and of (**M**) 300 μM BzATP. Neither the broad spectrum P2R agonist ATP (**I**) nor the $P2Y_1R$ specific agonist 2MeSADP (**J**) induced calcium rises in $P2Y_1R$-null GPCs loaded with Fluo-3-AM. Moreover, the $P2Y_{2/4}R$ agonist UTP (**K**), the broad spectrum P2XR agonist $\alpha\beta$MeATP (**L**) or the $P2X_7R$ agonist BzATP (**M**) did not increase intracellular calcium levels above 5% F/F_0.

of $P2Y_1R$-null neuroblasts did not induce further inhibition of neuronal migration (271 ± 14 μm; n=4 independent experiments).

Confirmation of expected loss of $P2Y_1Rs$ in $P2Y_1R$-null-derived cerebellar cells was obtained by immunocytochemistry and by functional assays. Immunostaining with anti-$P2Y_1R$ antibodies on WT and $P2Y_1R$-null explants confirmed the lack of expression in $P2Y_1R$-derived GCPs and their presence in WT cells (Figures 5A–5H). In accordance with the lack of immunoreactivity, no intracellular calcium changes were recorded following bath application of 1 μM of the broad spectrum P2R agonist ATP (431 cells; n=6 independent experiments) and 1 μM of the $P2Y_1R$-specific agonist 2MeSADP (218 cells; n=4 independent experiments). Also, similar to what was observed in WT cells, 1 μM UTP (a $P2Y_{2/4}$ receptor agonist; 100 cells; n=2 independent experiments), 1 μM $\alpha\beta$MeATP (a P2X receptor agonist; 118 cells; n=2 independent experiments), and 300 μM BzATP (a $P2X_7$

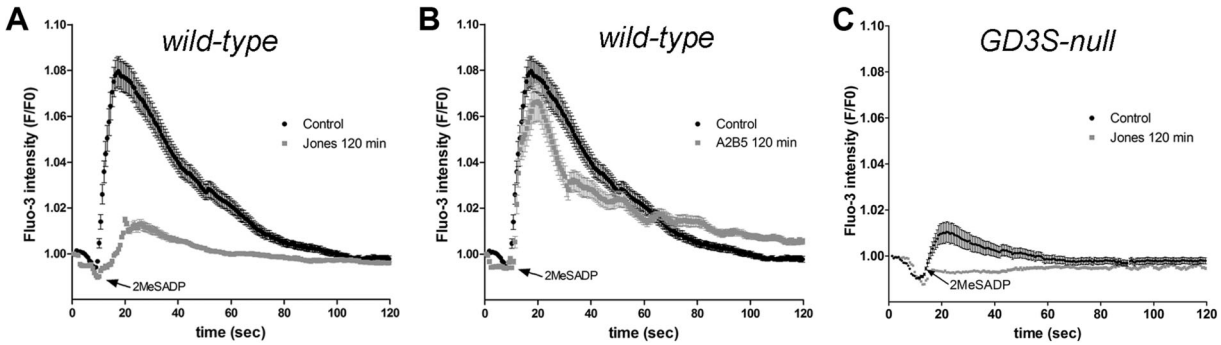

Figure 6 **Immunoblockade of 9acGD3 by J-Ab reduces activation of P2Y$_1$R on GCPs**
Graphs showing the time course of intracellular calcium changes induced by bath application of 1 μM 2MeSADP in the absence (black traces in **A** and **B**) and presence (light-grey trace in **A**) of Jones and (light-grey trace in **B**) of A2B5 antibodies for 2 h in GCPs. Data points represent means ± S.E.M. of at least 255 cells from at least three independent experiments.

receptor agonist; 250 cells; $n=3$ independent experiments) did not induce detectable changes in intracellular calcium levels in P2Y$_1$R-null GCPs (Figures 5I–5M).

Combined, these results indicate that spontaneous calcium oscillations recorded from GCPs are exclusively mediated by P2Y$_1$R activation and that deletion of these receptors is not accompanied by compensatory mechanisms involving the functional expression of other P2 receptors or alteration in the expression/distribution of the 9acGD3 (Figures 5A–5H).

Immunoblockade or deletion of 9-OacGD3 affects P2Y$_1$R-mediated calcium transients by reducing receptor surface expression

To evaluate the effect of J-Ab on GPC P2Y$_1$R-mediated calcium signalling, we measured 2MeSADP-induced calcium transients in cells acutely treated with J-Ab (1 ng/ml). Bath application of 1 μM 2MeSADP in J-Ab-treated cells resulted in GCP calcium transients with amplitudes similar to those recorded from J-Ab untreated cells (Jones: 1.080 ± 0.001; control: 1.079 ± 0.001; $n=5$ independent experiments). However, prolonged incubation (2 h) with J-Ab led to a reduction in P2Y$_1$R responsiveness. Under these conditions, both the percentage of responding cells and their calcium amplitudes were significantly reduced (5%: 15 of 300 cells showing 1.019 ± 0.002-fold increase in relative Fluo-3 intensity; $n=3$ independent experiments; $P<0.01$; grey trace in Figure 6A). A2B5 treatment for 2 h did not significantly alter calcium amplitudes or the percentage of cells responding to the P2Y$_1$R agonist (35%: 90 of 255 cells showing 1.070 ± 0.008-fold increase in relative Fluo-3 intensity; $n=3$ independent experiments; $P>0.05$; grey trace in Figure 6B) compared with untreated cells.

Evidence that the alteration of GCP P2Y$_1$R-mediated calcium signalling seen following prolonged exposure to J-Ab was not due to non-specific effects of the antibody came from experiments performed on GD3S-null cells. Similarly to the results obtained following GD3 immunoblockade, in GD3-null cells we also recorded a significant reduction in the amplitudes of 2MeSADP-induced calcium transients and in the number of responding cells (1.010 ± 0.004-fold increase in relative Fluo-3 intensity; 7%: 22 of 300 cells; three independent experiments; $P<0.01$; black trace in Figure 6C) compared with WT control cells (black trace in Figure 6A). Incubation of GD3S-null cells with J-Ab had no further effect on calcium amplitudes (0.994 ± 0.001-fold increase in relative Fluo-3 intensity) or on the percentage of cells responding to the agonist (4%: 11 of 260 cells; three independent experiments; $P>0.05$; grey trace in Figure 6C).

To gain insight into the nature of the inactivation of P2Y$_1$R following J-Ab treatment, we evaluated by confocal microscopy the distribution of 9acGD3 and P2Y$_1$R. For that, we transfected WT cerebellar explants with eGFP-P2Y$_1$R and analysed by high magnification of confocal images and *z*-reconstruction the distribution of these receptors in GCPs before and after incubation with Jones and A2B5 antibodies. In J-Ab untreated explants, eGFP-tagged P2Y$_1$ receptors were mainly distributed on the cell membrane (Figures 7A and 7B). Incubation for 2 h with 1 ng/ml Jones (Figure 7C) but not with A2B5 induced internalization of eGFP-P2Y$_1$R on migrated GCPs. Fluorescence intensity profile analyses (Figures 7D and 7E) of GCPs showed a significantly higher intracellular distribution of eGFP-P2Y$_1$R in Jones- (compare black and red traces in Figure 7D) but not in A2B5-treated cells (compare black and red traces in Figure 7E). Shorter time treatments with J-Ab (30 min) did not affect the distribution of P2Y$_1$R (data not shown).

Further evidence that P2Y$_1$R membrane expression depends on GD3 ganglioside came from similar experiments performed on WT and GD3 KO cerebellar neuroblasts immunostained with anti-P2Y$_1$ antibody. In contrast with WT neuroblasts where P2Y$_1$R immune reactivity was abundant at the cell surface, in GD3 KO cells, an intracellular distribution of these receptors was evident (Figure 7F). Fluorescence intensity profiles (Figure 7G) clearly show the different cellular distribution of P2Y$_1$R in both genotypes and a similar intracellular distribution in GD3 synthase KO and WT neuroblasts treated with J-Ab (compare Figures 7D and 7G).

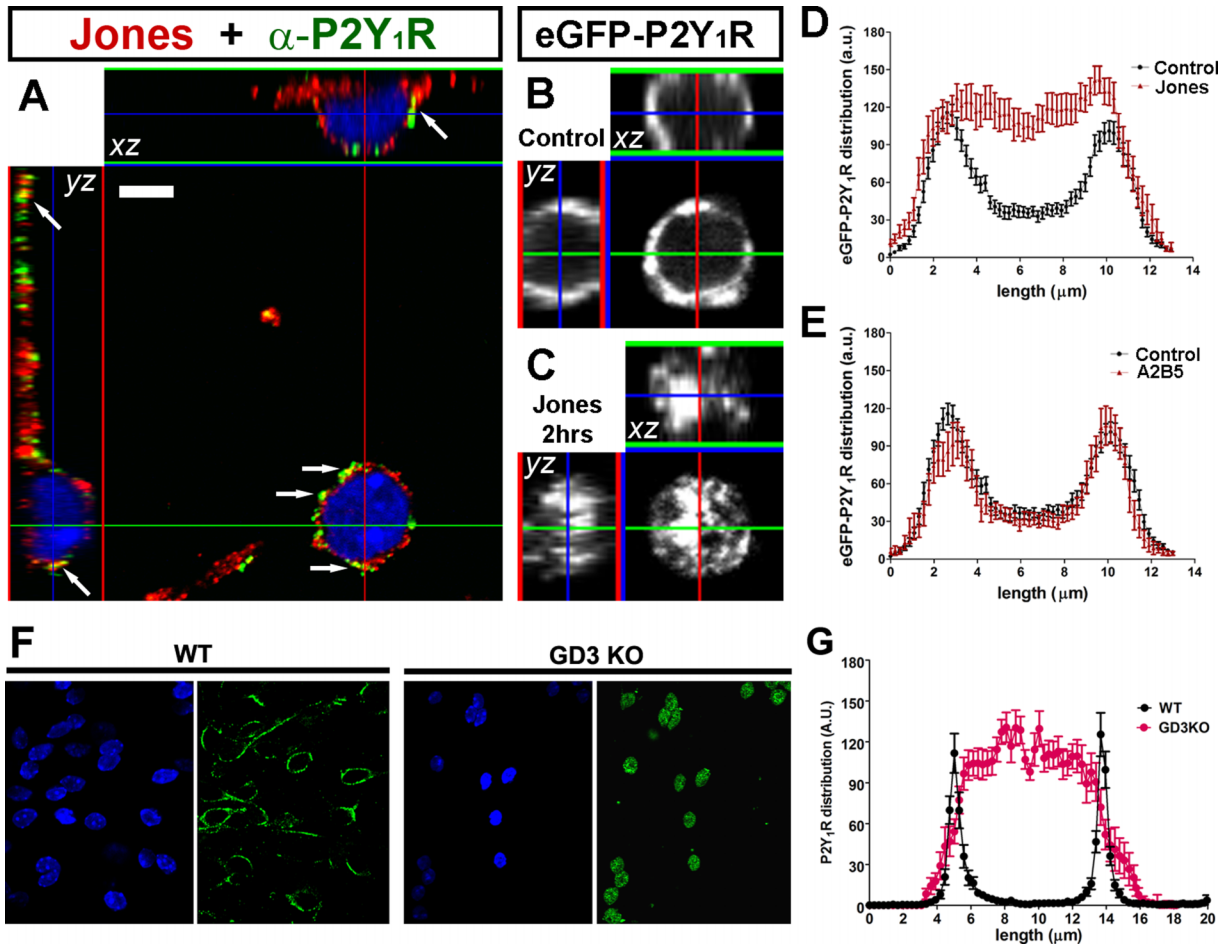

Figure 7 **Internalization of $P2Y_1Rs$ by Jones treatment**
Confocal images of fixed (**A**) and live (**B**, **C**) GCPs migrated from P6 WT mice explants. Double staining with Jones (red) and α-$P2Y_1R$ (green) antibodies showing a punctated expression of both antigens (**A**). Orthogonal views (*xz* and *yz*) through *z*-reconstruction confocal images showing in detail the distribution of both antigens around the cell body and neurites of migrated GCPs revealing a weak co-localization (yellow) between the ganglioside 9acGD3 and $P2Y_1R$ (arrows in **A**). Confocal images of eGFP-$P2Y_1R$-transfected GCPs before (**B**) and after (**A**) Jones incubation for 2 h. Analyses of fluorescence intensity profiles of eGFP-$P2Y_1R$ before (black traces) and after (red traces) Jones (**D**) and A2B5 (**E**) treatments for 2 h. (**F**) Confocal images of $P2Y_1R$ immunostaining obtained from WT and GD3 synthase null (GD3 KO) neuroblasts, showing the distinct cellular distribution of $P2Y_1R$; fluorescence profile plots of these receptors in the two genotypes are shown in (**G**). Each data point represents means ± S.E.M. of 56 (control), 28 (Jones) and 21 (A2B5) eGFP-$P2Y_1R$ transfected emigrated GCPs, and from 20 to 23 cells from WT and GD3 KO immunostained for $P2Y_1R$. Data are from three independent experiments.

DISCUSSION

Over the past two decades significant information has accumulated about molecules and signalling pathways implicated in the migration of GCPs in the developing cerebellum (Komuro and Yacubova, 2003; Chedotal, 2010). Among these signalling molecules, the 9acGD3 gangliosides have been reported to play an important role during cerebellar neuroblast migration (Santiago et al., 2001, 2004); however, the mechanism by which this type of ganglioside contributes to this process is not totally resolved. Studies have suggested that the interactions of the ganglioside 9acGD3 with β_1 integrin and vinculin at points of contact of axonal growth cones are important for growth cone motility (Negreiros et al., 2003). This was evidenced in experiments in which immunoblockade of the 9acGD3 ganglioside with the J-Ab induced microtubule depolymerization and arrest of growth cone motility of dorsal root ganglia neurons (Mendez-Otero and Friedman, 1996; Araujo et al., 1997).

Besides adhesion molecules, intracellular calcium signals have been implicated in progenitor cell migration, with the frequency of calcium transients being correlated with the migration rate (Scemes et al., 2003; Komuro and Kumada, 2005). Evidence for a role of calcium transients and adenosine nucleotide signalling through P2Rs in progenitor cell migration has been described by various groups. For instance, migration of glial progenitor cells derived from mouse embryonic cortical neurospheres and explants was shown to be regulated by intracellular Ca^{2+} oscillations driven by ATP activation of $P2Y_1R$ (Scemes et al., 2003; Striedinger et al.,

2007). In addition, in the mouse developing neocortex, the interkinetic nuclear migration in the ventricular zone and the migration of intermediate neuronal progenitors from the ventricular surface to the subventricular zone was shown to be dependent on intercellular ATP signalling through activation of the neuronal $P2Y_1R$ (Liu et al., 2008, 2010). In the cerebellum, the rate of GCP migration is correlated with Ca^{2+} transients (Komuro and Rakic, 1996) that have been reported to be modulated by activation of NMDA (*N*-methyl-D-aspartate)- and somatostatin-receptors (Komuro and Rakic, 1993; Yacubova and Komuro, 2002).

The direct involvement of purinergic-driven calcium transients in GCP migration, however, has not been previously described. Here, we provide strong evidence for the presence of $P2Y_1R$ in GCPs. Using pharmacological tools, immunocytochemistry and transgenic mice lacking these receptors, we show here for the first time that explant-emigrated GCPs express functional $P2Y_1Rs$ and that the activation of these purinergic receptors by extracellular ATP generates Ca^{2+} transients. Moreover, it is shown here that blockade of these receptors with a specific antagonist or the deletion of $P2Y_1R$ reduces the frequency of calcium oscillations and the rate of migration of these cells.

In line with our results, a previous study performed on developing cerebellum has suggested a role of $P2Y_1Rs$ in Bergman glia-guided granule cell migration (Amadio et al., 2007). These authors found that at early stages (postnatal day 7) of cerebellar development the expression of $P2Y_1R$ was prominent at the interface between migrating granule cells and Bergman glia, while at postnatal day 21, when neuronal migration is completed, $P2Y_1Rs$ were mainly found in Purkinje cell body ramifications and on synaptic varicosities, and were absent from Bergman glia (Amadio et al., 2007).

The major finding of the present study relates to the unexpected influence of a ganglioside on $P2Y_1R$-mediated calcium signalling and cell migration. Here, we provide experimental evidence that immunoblockade of 9acGD3 arrests the migration of mouse GCPs by affecting $P2Y_1R$ signalling. The immunoblockade of the 9acGD3 is shown to inhibit $P2Y_1R$-driven spontaneous intracellular calcium oscillations of GCPs and to be correlated with the internalization of the $P2Y_1R$, as revealed by Jones-induced internalization of eGFP-$P2Y_1R$ on transfected GCPs, and by immunostaining of native $P2Y_1R$ in GD3 synthase null mice.

Although further studies are necessary to completely resolve the mechanisms involved in Jones-induced $P2Y_1R$ internalization, it is likely that cell adhesion molecules and cytoskeletal elements participate in this process. For instance, acto-myosin motors which are coordinated by the polarity protein Par6α in migrating GCPs have been reported to participate in the regulation of somal and centrosomal forward movements (Solecki et al., 2004, 2009). Moreover, previous studies have indicated that plasma membrane-bound P2Rs interact with integrin receptors and cytoskeleton components to regulate chemotaxis and migration in various cell types (Koles et al., 2008; Neary and Zimmermann, 2009). For instance, $P2Y_{12}R$-mediated integrin-β1 activation is involved in directional process extension by microglia in brain (Ohsawa et al., 2010). Therefore it will be interesting to investigate whether Jones immunoblockade interferes with transmembrane signals via purinergic-driven integrin activation and disarrangement of the cytoskeletal machinery in migrating GCPs.

The possibility, however, that the antibody Jones could also recognize other proteins such as β_1 integrin receptors expressed by cerebellar GCPs *in vitro* (Yang et al., 2007) seems unlikely. First, it was previously shown that J-Ab fails to recognize any bands in SDS-polyacrylamide gels from protein extracts of different regions of the developing brain, including the neonatal cerebellum (Constantine-Paton et al., 1986; Schlosshauer et al., 1988). Secondly, Jones-reactive antigens were prominent in chloroform/methanol extracts of the same tissues and enzymatic treatments indicated that the Jones epitope was sensitive to neuraminidase but not to proteases, thus, indicating the glycolipid origin of all Jones-reactive antigens (Schlosshauer et al., 1988). Finally, as shown here, the lack of Jones immune reactivity in GD3S-null explants and the absence of effect of this antibody on the migration and calcium signalling of GD3S-null neuroblasts further speak in favour of the specificity of the J-Ab in recognizing 9acGD3. This is in contrast with a previous study suggesting that J-Ab, besides targeting molecules other than the GD3 ganglioside, reduced GD3S-null neuroblast migration to a similar extent as in WT cells (Yang et al., 2007). Although we do not have an explanation for these discrepancies, it is possible that they could have resulted from the use of distinct culture conditions and analysis methods from the ones used here.

Interestingly, however, as for most ganglioside knockout mice so far tested, GD3S-null mice do not have a striking phenotype (Okada et al., 2002) at least at adult ages, although (GD3+GM2/GD2) double knockout mice do (Ohmi et al., 2011). The lack of phenotype of single knockouts is explained by compensatory mechanisms, one of which being the alternate pathway for ganglioside synthesis (reviewed in Yu et al., 2012). Alternatively, or in addition, developmental changes in membrane lipid composition, such as those related to the synthesis of complex gangliosides, can lead to the remodelling of membrane microdomains and their associated signalling molecules (Cantu et al., 2011; Ohmi et al., 2011; Yu et al., 2012). In this context, it is interesting that in post-migratory neurons, a time point when simple gangliosides such as the GM3, GD3 and 9-OacGD3 are down regulated, synaptic $P2Y_1Rs$ are mainly found in flotillin lipid rafts or are associated with GM1, a complex ganglioside (Amadio et al., 2007).

In summary, we provide strong evidence in this study using genetic, pharmacological, enzymatic and immunological interventions that the ganglioside 9-OacGD3 reduces neuroblast migration by decreasing $P2Y_1R$-mediated spontaneous calcium oscillations, due to receptor internalization. This novel mechanism by which $P2Y_1$ receptor distribution and

function can be modulated, likely serves as an efficient way to switch off signalling pathways involved in neuroblast migration.

ACKNOWLEDGEMENTS

We appreciate the discussions and helpful comments provided by Dr David C. Spray. We acknowledge the technical assistance of Mrs Aisha Cordero and Mr Naman Patel with animal husbandry.

FUNDING

This work was supported by CAPES [grant number bex#4143-09-4 (fellowship to M.F.S.)], by NINDS-NIH [grant number RO1-NS054225 (to E.S.)], and by NICHD-NIH [grant number 1P30HD071593-01].

REFERENCES

Adams NC, Tomoda T, Cooper M, Dietz G, Hatten ME (2002) Mice that lack astrotactin have slowed neuronal migration. Development 129:965–972.

Agresti C, Meomartini ME, Amadio S, Ambrosini E, Volonte C, Aloisi F, Visentin S (2005a) ATP regulates oligodendrocyte progenitor migration, proliferation, and differentiation: involvement of metabotropic P2 receptors. Brain Res Brain Res Rev 48:157–165.

Agresti C, Meomartini ME, Amadio S, Ambrosini E, Serafini B, Franchini L, Volonte C, Aloisi F, Visentin S (2005b) Metabotropic P2 receptor activation regulates oligodendrocyte progenitor migration and development. Glia 50:132–144.

Amadio S, Vacca F, Martorana A, Sancesario G, Volonte C (2007) $P2Y_1$ receptor switches to neurons from glia in juvenile versus neonatal rat cerebellar cortex. BMC Dev Biol 7:77.

Araujo H, Menezes M, Mendez-Otero R (1997) Blockage of 9-O-acetyl gangliosides induces microtubule depolymerization in growth cones and neurites. Eur J Cell Biol 72:202–213.

Bates B, Rios M, Trumpp A, Chen C, Fan G, Bishop JM, Jaenisch R (1999) Neurotrophin-3 is required for proper cerebellar development. Nat Neurosci 2:115–117.

Ben-Arie N, Bellen HJ, Armstrong DL, McCall AE, Gordadze PR, Guo Q, Matzuk MM, Zoghbi HY (1997) Math1 is essential for genesis of cerebellar granule neurons. Nature 390:169–172.

Borghesani PR, Peyrin JM, Klein R, Rubin J, Carter AR, Schwartz PM, Luster A, Corfas G, Segal RA (2002) BDNF stimulates migration of cerebellar granule cells. Development 129:1435–1442.

Cameron DB, Galas L, Jiang Y, Raoult E, Vaudry D, Komuro H (2007) Cerebellar cortical-layer-specific control of neuronal migration by pituitary adenylate cyclase-activating polypeptide. Neuroscience 146:697–712.

Cantu L, Del Favero E, Sonnino S, Prinetti A (2011) Gangliosides and the multiscale modulation of membrane structure. Chem Phys Lip 164:796–810.

Chedotal A (2010) Should I stay or should I go?Becoming a granule cell. Trends Neuroscie 33:163–172.

Constantine-Paton M, Blum AS, Mendez-Otero R, Barnstable CJ (1986) A cell surface molecule distributed in a dorsoventral gradient in the perinatal rat retina. Nature 324:459–462.

Eisenbarth GS, Walsh FS, Nirenberg M (1979) Monoclonal antibody to a plasma membrane antigen of neurons. Proc Natl Acad Sci USA 76:4913–4917.

Hakomori S (2002) Inaugural article: the glycosynapse. Proc Natl Acad Sci USA 99:225–232.

Hatten ME (1999) Central nervous system neuronal migration. Annu Rev Neurosci 22:511–539.

Herculano-Houzel S (2010) Coordinated scaling of cortical and cerebellar numbers of neurons. Front Neuroanat 4:12.

Hervas C, Perez-Sen R, Miras-Portugal MT (2003) Coexpression of functional P2X and P2Y nucleotide receptors in single cerebellar granule cells. J Neuroscie Res 73:384–399.

Hockberger PE, Tseng HY, Connor JA (1987) Immunocytochemical and electrophysiological differentiation of rat cerebellar granule cells in explant cultures. J Neurosci 7:1370–1383.

Hong SE, Shugart YY, Huang DT, Shahwan SA, Grant PE, Hourihane JO, Martin ND, Walsh CA (2000) Autosomal recessive lissencephaly with cerebellar hypoplasia is associated with human RELN mutations. Nat Genet 26:93–96.

Husmann K, Faissner A, Schachner M (1992) Tenascin promotes cerebellar granule cell migration and neurite outgrowth by different domains in the fibronectin type III repeats. J Cell Biol 116:1475–1486.

Ito M (2006) Cerebellar circuitry as a neuronal machine. Prog Neurobiol 78:272–303.

Kawai H, Allende ML, Wada R, Knon M, Sango K, Deng C, Miyakawa T, Crawley JN, Werth N, Bierfreund U et al. (2001) Mice expressing only monosialoganglioside GM3 exhibit lethal audiogenic seizures. J Biol Chem 276:6885–6888.

Koles L, Gerevich Z, Oliveira JF, Zadori ZS, Wirkner K and Illes P (2008) Interaction of P2 purinergic receptors with cellular macromolecules. Naunyn Schmiedebergs Arch Pharmacol 377:1–33.

Komuro H, Rakic P (1993) Modulation of neuronal migration by NMDA receptors. Science 260:95–97.

Komuro H, Rakic P (1996) Intracellular Ca^{2+} fluctuations modulate the rate of neuronal migration. Neuron 17:275–285.

Komuro H, Rakic P (1998) Orchestration of neuronal migration by activity of ion channels, neurotransmitter receptors, and intracellular Ca^{2+} fluctuations. J Neurobiol 37:110–130.

Komuro H, Yacubova E (2003) Recent advances in cerebellar granule cell migration. Cell Mol Life Sci 60:1084–1098.

Komuro H, Kumada T (2005) Ca^{2+} transients control CNS neuronal migration. Cell Calcium 37:387–393.

Kumada T, Komuro H (2004) Completion of neuronal migration regulated by loss of Ca^{2+} transients. Proc Natl Acad Sci USA 101:8479–8484.

Ledeen RW, Yu RK (1982) Gangliosides: structure, isolation, and analysis. Methods Enzymol 83:139–191.

Li S, Qiu F, Xu A, Price SM, Xiang M (2004) Barhl1 regulates migration and survival of cerebellar granule cells by controlling expression of the neurotrophin-3 gene. J Neurosci 24:3104–3114.

Liu X, Hashimoto-Torii K, Torii M, Haydar TF, Rakic P (2008) The role of ATP signaling in the migration of intermediate neuronal progenitors to the neocortical subventricular zone. Proc Natl Acad Sci USA 105:11802–11807.

Liu X, Hashimoto-Torii K, Torii M, Ding C, Rakic P (2010) Gap junctions/hemichannels modulate interkinetic nuclear migration in the forebrain precursors. J Neurosci 30:4197–4209.

Mendez-Otero R, Friedman JE (1996) Role of acetylated gangliosides on neurite extension. Eur J Cell Biol 71:192–198.

Mendez-Otero R, Schlosshauer B, Barnstable CJ, Constantine-Paton M (1988) A developmentally regulated antigen associated with neural cell and process migration. J Neurosci 8:564–579.

Nagata I, Nakatsuji N (1990) Granule cell behavior on laminin in cerebellar microexplant cultures. Brain Res Dev Brain Res 52:63–73.

Neary JT, Zimmermann H (2009) Trophic functions of nucleotides in the central nervous system. Trends Neuroscie 32:189–198.

Negreiros EM, Leao AC, Santiago MF, Mendez-Otero R (2003) Localization of ganglioside 9-O-acetyl GD3 in point contacts of neuronal growth cones. J Neurobiol 57:31–37.

Ngamukote S, Yanagisawa M, Ariga T, Ando S, Yu RK (2007) Developmental changes of glycosphingolipids and expression of glycogenes in mouse brains. J Neurochem 103:2327–2341.

O'Shea KS, Rheinheimer JS, Dixit VM (1990) Deposition and role of thrombospondin in the histogenesis of the cerebellar cortex. J Cell Biol 110:1275–1283.

Ohmi Y, Tajima O, Ohkawa Y, Sugira Y, Furukawa K, Furukawa K (2011) Gangliosides are essential in the protection of inflammation and neurodegeneration via maintenance of lipid rafts: elucidation by a series of ganglioside-deficient mutant mice. J Neurochem 116:926–935.

Ohmi Y, Ohkawa Y, Yamauchi Y, Tajima O, Furukawa K, Furukawa K (2012) Essential roles of gangliosides in the formation and maintenance of membrane microdomains in brain tissues. Neurochem Res 37:1185–1191.

Ohsawa K, Irino Y, Sanagi T, Nakamura Y, Suzuki E, Inoue K, Kohsaka S (2010) $P2Y_{12}$ receptor-mediated integrin-beta1 activation regulates microglial process extension induced by ATP. Glia 58:790–801.

Okada M, Itoh M, Haraguchi M, Okajima T, Inoue M, Oishi H, Matsuda Y, Iwamoto T, Kawano T, Fukumoto S, Miyazaki H, Furukawa K, Aizawa S, Furukawa K (2002) b-series ganglioside deficiency exhibits no definite

changes in the neurogenesis and the sensitivity to Fas-mediated apoptosis but impairs regeneration of the lesioned hypoglossal nerve. J Biol Chem 277:1633–1636.

Rakic P (1971) Neuron–glia relationship during granule cell migration in developing cerebellar cortex. A Golgi and electronmicroscopic study in *Macacus Rhesus*. J Comp Neurol 141:283–312.

Santiago MF, Costa MR, Mendez-Otero R (2004) Immunoblockage of 9-O-acetyl GD3 ganglioside arrests the *in vivo* migration of cerebellar granule neurons. J Neurosci 24:474–478.

Santiago MF, Berredo-Pinho M, Costa MR, Gandra M, Cavalcante LA, Mendez-Otero R (2001) Expression and function of ganglioside 9-O-acetyl GD3 in postmitotic granule cell development. Mol Cell Neurosci 17:488–499.

Santiago MF, Liour SS, Mendez-Otero R, Yu RK (2005) Glial-guided neuronal migration in P19 embryonal carcinoma stem cell aggregates. J Neurosci Res 81:9–20.

Scemes E, Duval N, Meda P (2003) Reduced expression of $P2Y_1$ receptors in connexin43-null mice alters calcium signaling and migration of neural progenitor cells. J Neurosci 23:11444–11452.

Schlosshauer B, Blum AS, Mendez-Otero R, Barnstable CJ, Constantine-Paton M (1988) Developmental regulation of ganglioside antigens recognized by the Jones antibody. J Neurosci 8:580–592.

Schwartz PM, Borghesani PR, Levy RL, Pomeroy SL, Segal RA (1997) Abnormal cerebellar development and foliation in $BDNF^{-/-}$ mice reveals a role for neurotrophins in CNS patterning. Neuron 19:269–281.

Solecki DJ, Model L, Gaetz J, Kapoor TM, Hatten ME (2004) Par6alpha signaling controls glial-guided neuronal migration. Nat Neurosci 7:1195–1203.

Solecki DJ, Trivedi N, Govek EE, Kerekes RA, Gleason SS, Hatten ME (2009) Myosin II motors and F-actin dynamics drive the coordinated movement of the centrosome and soma during CNS glial-guided neuronal migration. Neuron 63:63–80.

Striedinger K, Meda P, Scemes E (2007) Exocytosis of ATP from astrocyte progenitors modulates spontaneous Ca^{2+} oscillations and cell migration. Glia 55:652–662.

Taube S, Perry JW, Yetming K, Patel SP, Auble H, Shu L, Nawar HF, Lee CH, Connell TD, Shayman JA, Wobus CE (2009) Ganglioside-linked terminal sialic acid moieties on murine macrophages function as attachment receptors for murine noroviruses. J Virol 83:4092–4101.

Vaudry D, Gonzalez BJ, Basille M, Fournier A, Vaudry H (1999) Neurotrophic activity of pituitary adenylate cyclase-activating polypeptide on rat cerebellar cortex during development. Proc Natl Acad Sci USA 96:9415–9420.

Wilson PM, Fryer RH, Fang Y, Hatten ME (2010) Astn2, a novel member of the astrotactin gene family, regulates the trafficking of ASTN1 during glial-guided neuronal migration. J Neurosci 30:8529–8540.

Yacubova E, Komuro H (2002) Stage-specific control of neuronal migration by somatostatin. Nature 415:77–81.

Yang CR, Liour SS, Dasgupta S, Yu RK (2007) Inhibition of neuronal migration by JONES antibody is independent of 9-O-acetyl GD3 in GD3-synthase knockout mice. J Neurosci Res 85:1381–1390.

Yu RK, Nakatani Y, Yanagisawa M (2009) The role of glycosphingolipid metabolism in the developing brain. J Lipid Res 50 Suppl:S440–445.

Yu RK, Tsai YT, Ariga T (2012) Functional roles of gangliosides in neurodevelopment: an overview. Neurochem Res 37:1230–1244.

Zheng C, Heintz N, Hatten ME (1996) CNS gene encoding astrotactin, which supports neuronal migration along glial fibers. Science 272:417–419.

Received 16 May 2012/6 July 2012; accepted 13 July 2012

Published as Immediate Publication 15 August 2012, doi 10.1042/AN20120035